Supplementary information

Aptamer Immobilization on Amino Functionalized Metal Organic Frameworks: An Ultrasensitive Platform for Electrochemical Diagnostic of *Escherichia coli O157:H7*

Saeed Shahrokhian[1,2*], Saba Ranjbar[1]

[1]*Department of Chemistry, Sharif University of Technology, Tehran 11155-9516, Iran*

[2]*Institute for Nanoscience and Nanotechnology, Sharif University of Technology, Tehran, Iran*

TABLE AND FIGURE CAPTIONS

Scheme S1. Schematic illustration of interaction between PANI/MOF and amine modified aptamer with GA as cross linking agent.

Table S1. Comparison the analytical performance of presented electrochemical aptasensor for *E. coli O157:H7* detection.

Table S2. Recovery tests for *E. coli O157:H7* in different water samples.

Fig S1. The effect of PBS in DPV response of 20 μM MB (in 20 mM Tris-HCl, pH 7.4) for aptasensor, (a) aptasensor incubated in 20 μM MB, (b) aptasensor incubated in 20 μM MB and immersed in PBS (0.1M, pH= 7.4) and (c) aptasensor incubated in 20 μM MB, immersed in PBS (0.1M, pH= 7.4) and incubated in 2.1×10^4 CFU mL^{-1} *E. coli O157:H7*.

Fig S2. Secondary structure of *E. coli O157:H7* DNA aptamer predicted by mfold program.

Fig S3. Interaction of aptamer with some *E. coli O157:H7* specific epitopes determined with HEX.8.0.0 software (A) metalloprotein, (B) UPF0209 protein and (C) effector protein.

Fig S4. EDS analysis of (A) Cu-MOF, (B) PANI and (C) PANI/MOF.

Fig S5. (A) Results of cyclic voltammograms (Scan rate, 100 mVs^{-1}) and (B) Nyquist plots of 0.1 M KCl containing 5 mM $Fe(CN)_6^{3-/4-}$ in GA immobilization step.

Fig S6. (A) DPV signal for 20 μM of MB at Apt/GA/PANI/GCE, (B) bar chart of peak current change in presence and absence of MOF, (C) DPV signal for 20 μM of MB at Apt/PANI/MOF/GCE and (D) bar chart of peak current change in presence and absence of GA.

Fig S7. The plot of $\Delta I_{p,\ MB}$ obtained with DPV technique for 20 μM MB versus PANI/MOF suspension volume in presence of 2.1×10^4 CFU mL^{-1} *E. coli O157:H7*.

Fig S8. (A) DPV signal recorded for aptasensor at various MB capture time and (B) the plot of $I_{p,\ MB}$ versus MB capture time.

Fig S9. (A) DPV signal recorded for aptasensor at various MB concentrations and (B) the plot of $I_{p,\ MB}$ versus MB concentration.

Fig S10. The plot of $\Delta I_{p,\ MB}$ obtained with DPV technique for 20 μM MB versus *E. coli O157:H7* (2.1×10^4 CFU mL^{-1}).

Fig S11. Bar chart for illustrate the regeneration of aptasensor in presence of 2M NaCl.

Fig S12. Evaluation the selectivity of purposed aptasensor for *E. coli O157:H7* compared to the other bacteria strains.

Fig S13. Images of LB agar plates containing cultured *E. coli O157:H7*.

Fig S14. (A) FESEM images and (B) EDS analysis for synthesized AgNPs.

Fig S15. Optical microscope images of (a) *E. coli O157:H7*, (b) AgNPs treated *E. coli O157:H7* and (c) ampicillin treated *E. coli O157:H7*.

Fig S16. DLS analyses of (a) monodispersed AgNPs and (b) aggregated AgNPs with *E. coli O157:H7*.

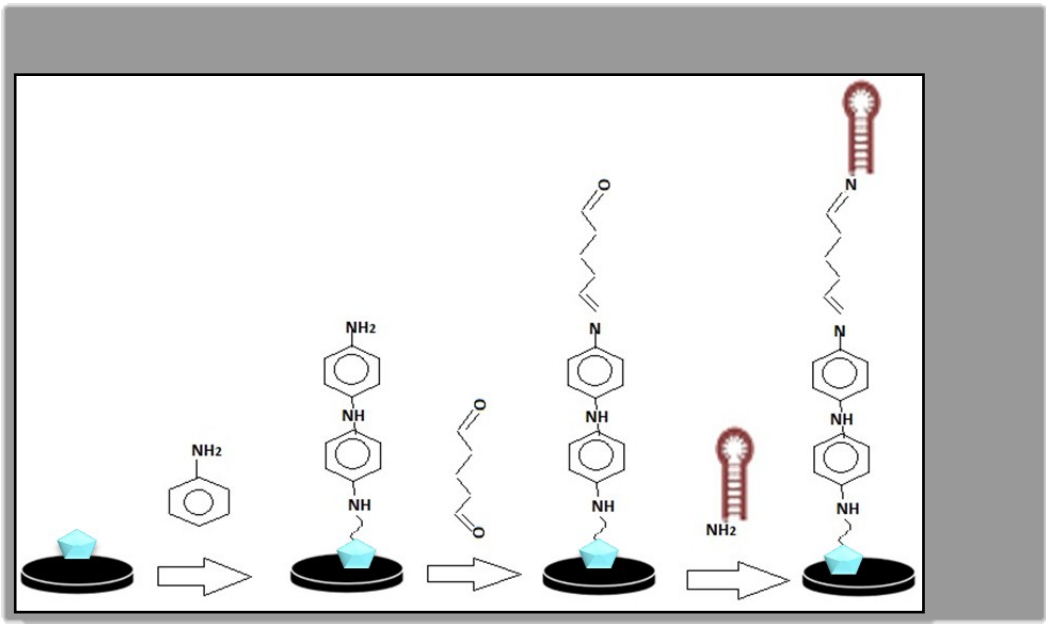

Scheme S1

Table S1

Purposed Biosensor	Detection Method	LDR CFU mL^{-1}	LOD CFU mL^{-1}	Analyze Time (min)	Reference
Aptamer/ SWCNT	Potentiometric	$1 – 10^3$	1	NR	24
AgBrNPs/3DNGH	Electrochemiluminesence	0.5-500	0.17	40	37
Aptamer/3D-IDEA	Impedimetric	10^1 - 10^6	2.9×10^2	30	38
Aptamer/PANI/MOF/GCE	Differential pulse voltammetry	2.1×10^1-2.1×10^7	2	40	This work

LDR: Linear dynamic range, LOD: Limit of detection, SWCNT: Single-walled carbon nanotube, 3D-IDEA: three-dimensional interdigitated electrode array, AgBrNPs: AgBr nanoparticles, 3DNGH: 3D nitrogen-doped graphene hydrogel, NR: not reported

Table S2

Sample	Spiked (CFU mL^{-1})	Found (CFU mL^{-1}) [a]	RSD (%) (n=3)	Recovery (%)
Tap Water	2.1×10^3	2.38×10^3	4.94	113.6
Mineral Water	2.1×10^3	2.00×10^3	2.57	95.3
Well Water	2.1×10^3	1.80×10^3	10.7	87.0
Paddy Water	2.1×10^3	1.54×10^3	2.15	73.2

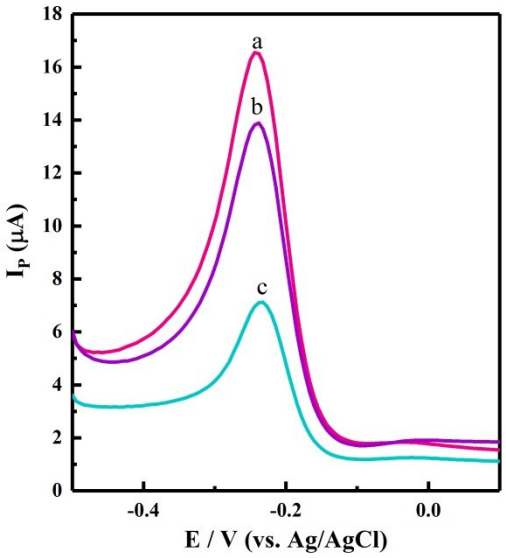

Fig. S1

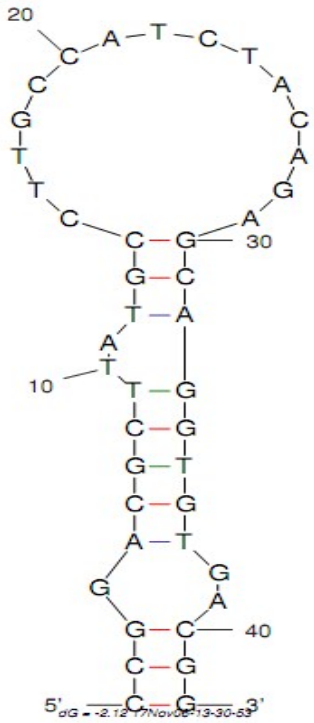

Fig. S2

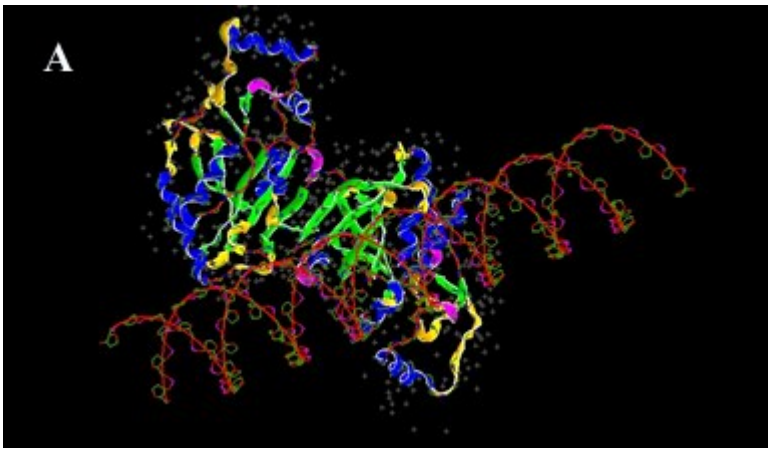

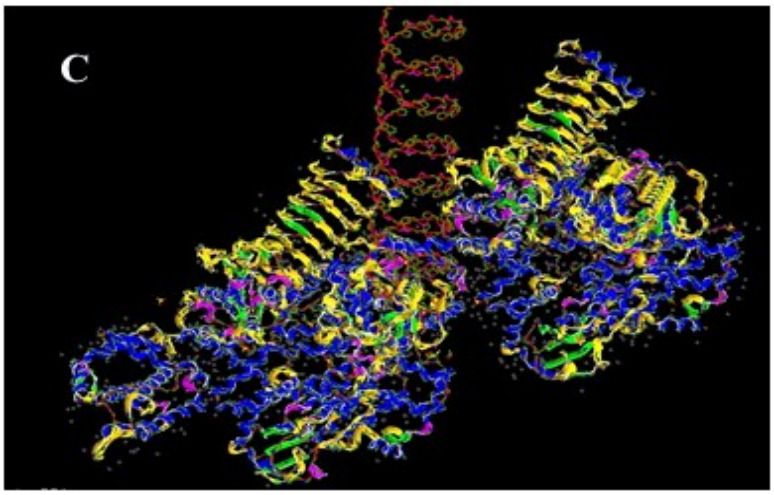

Fig. S3

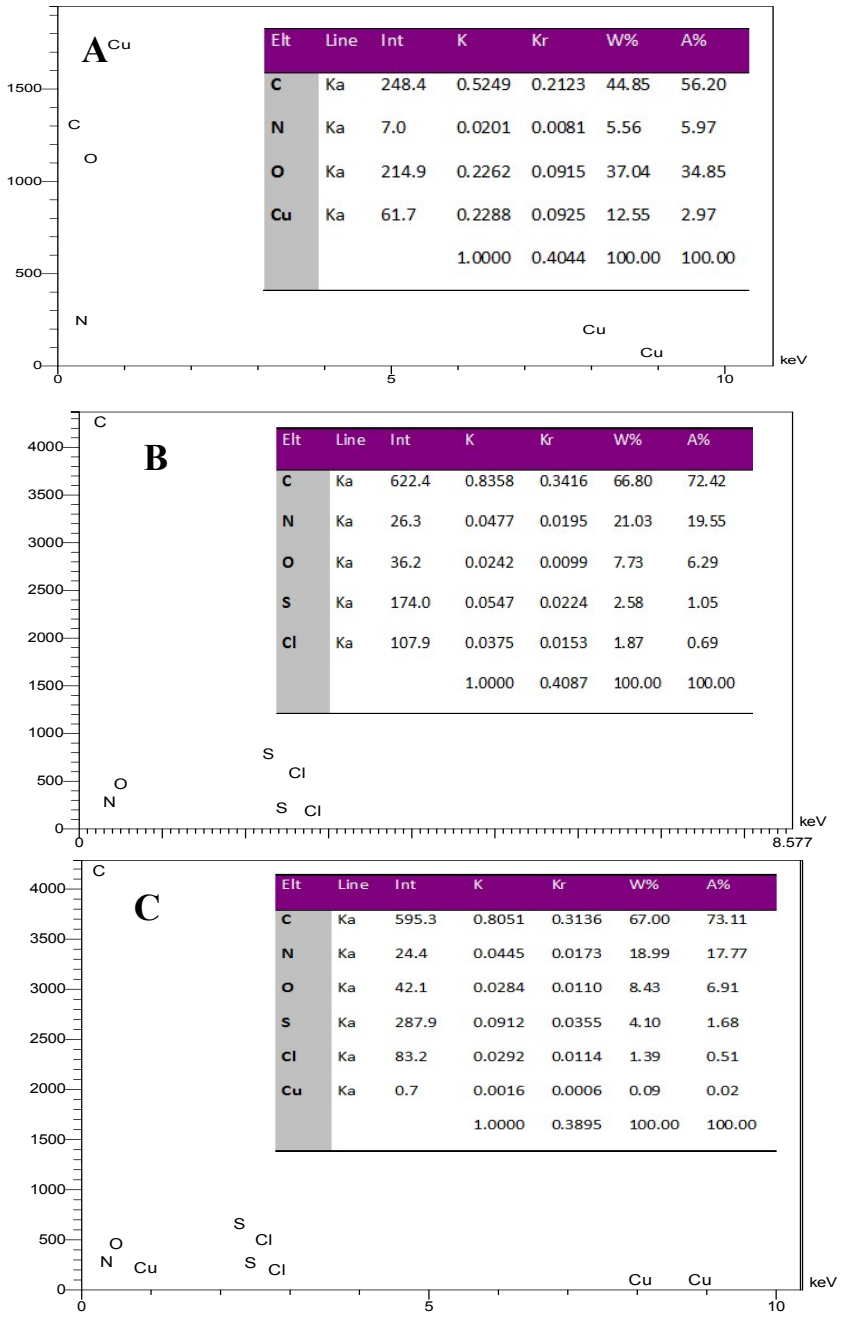
A
Cu
C
O
N
Cu
Cu
keV
Elt Line Int K Kr W% A%
C Ka 248.4 0.5249 0.2123 44.85 56.20
N Ka 7.0 0.0201 0.0081 5.56 5.97
O Ka 214.9 0.2262 0.0915 37.04 34.85
Cu Ka 61.7 0.2288 0.0925 12.55 2.97
1.0000 0.4044 100.00 100.00
B
C
S
Cl
O
N
S
Cl
keV
8.577
Elt Line Int K Kr W% A%
C Ka 622.4 0.8358 0.3416 66.80 72.42
N Ka 26.3 0.0477 0.0195 21.03 19.55
O Ka 36.2 0.0242 0.0099 7.73 6.29
S Ka 174.0 0.0547 0.0224 2.58 1.05
Cl Ka 107.9 0.0375 0.0153 1.87 0.69
1.0000 0.4087 100.00 100.00
C
S
Cl
O
N
Cu
S
Cl
Cu
Cu
keV
Elt Line Int K Kr W% A%
C Ka 595.3 0.8051 0.3136 67.00 73.11
N Ka 24.4 0.0445 0.0173 18.99 17.77
O Ka 42.1 0.0284 0.0110 8.43 6.91
S Ka 287.9 0.0912 0.0355 4.10 1.68
Cl Ka 83.2 0.0292 0.0114 1.39 0.51
Cu Ka 0.7 0.0016 0.0006 0.09 0.02
1.0000 0.3895 100.00 100.00

Fig. S4

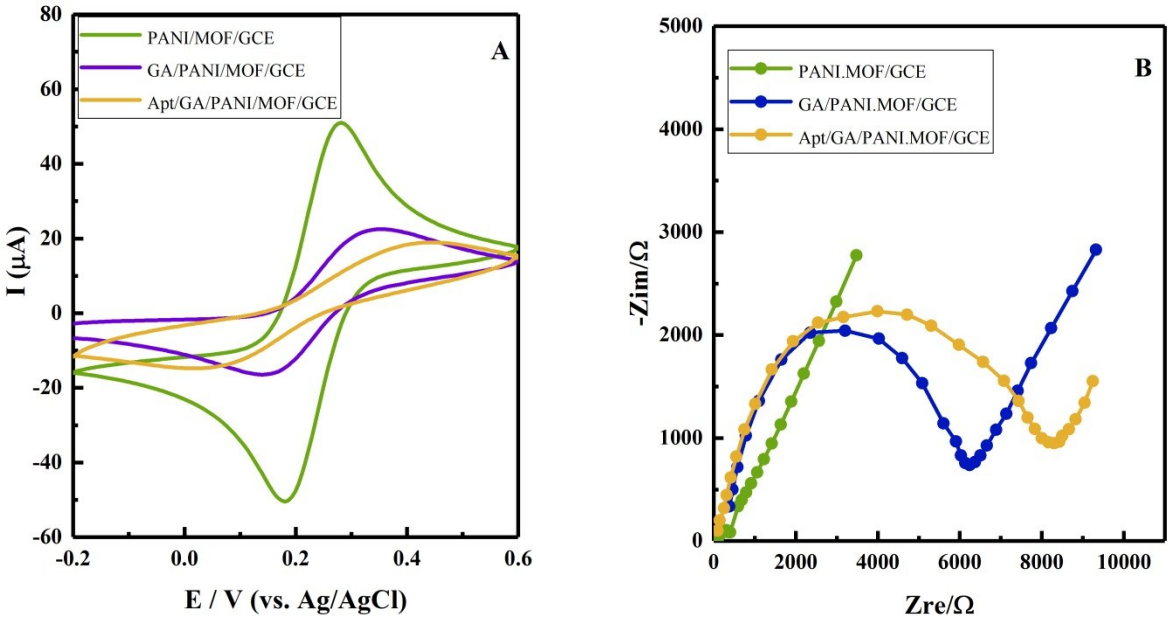
A
PANI/MOF/GCE
GA/PANI/MOF/GCE
Apt/GA/PANI/MOF/GCE
I (μA)
E / V (vs. Ag/AgCl)
B
PANI.MOF/GCE
GA/PANI.MOF/GCE
Apt/GA/PANI.MOF/GCE
-Zim/Ω
Zre/Ω

Fig. S5

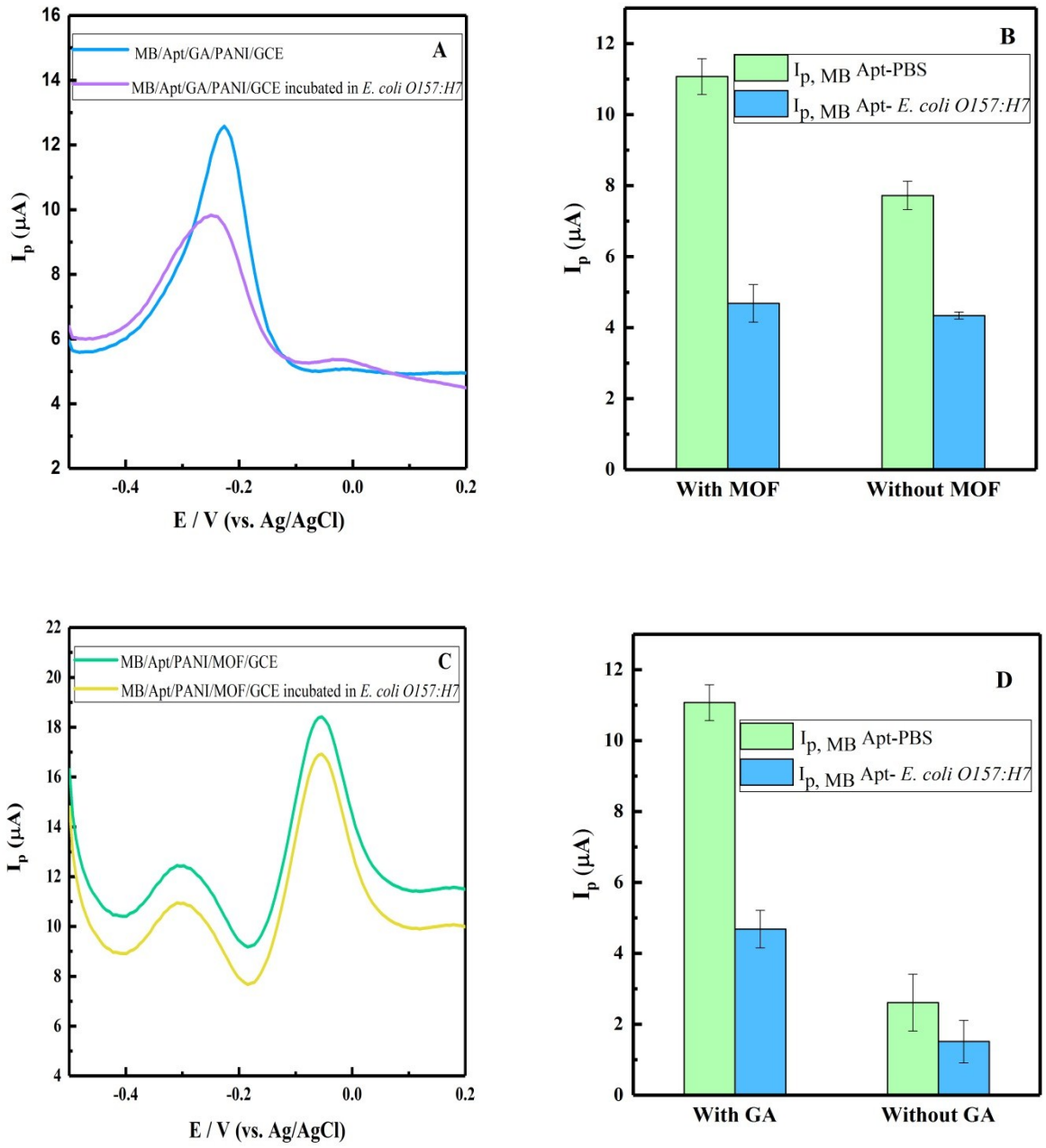
A
MB/Apt/GA/PANI/GCE
MB/Apt/GA/PANI/GCE incubated in E. coli O157:H7
I_p (μA)
E / V (vs. Ag/AgCl)
B
I_p, MB Apt-PBS
I_p, MB Apt- E. coli O157:H7
With MOF
Without MOF
C
MB/Apt/PANI/MOF/GCE
MB/Apt/PANI/MOF/GCE incubated in E. coli O157:H7
D
With GA
Without GA

Fig. S6

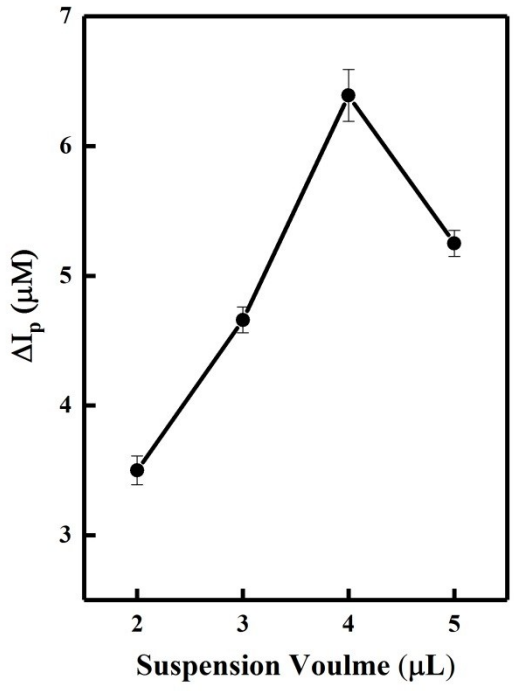

Fig. S7

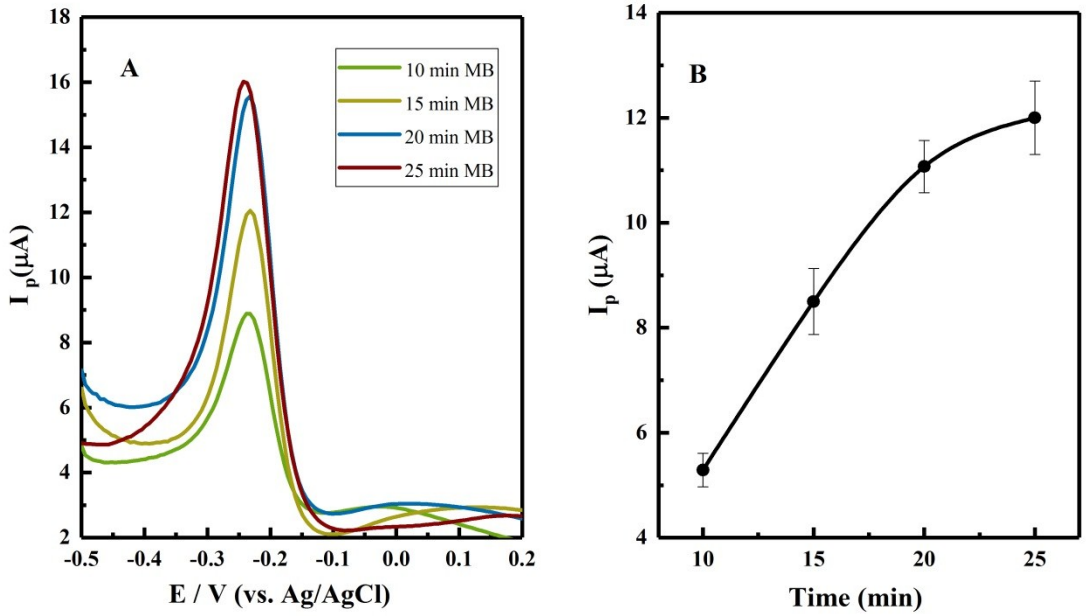
A
10 min MB
15 min MB
20 min MB
25 min MB
I p(μA)
E / V (vs. Ag/AgCl)
B
I p (μA)
Time (min)

Fig. S8

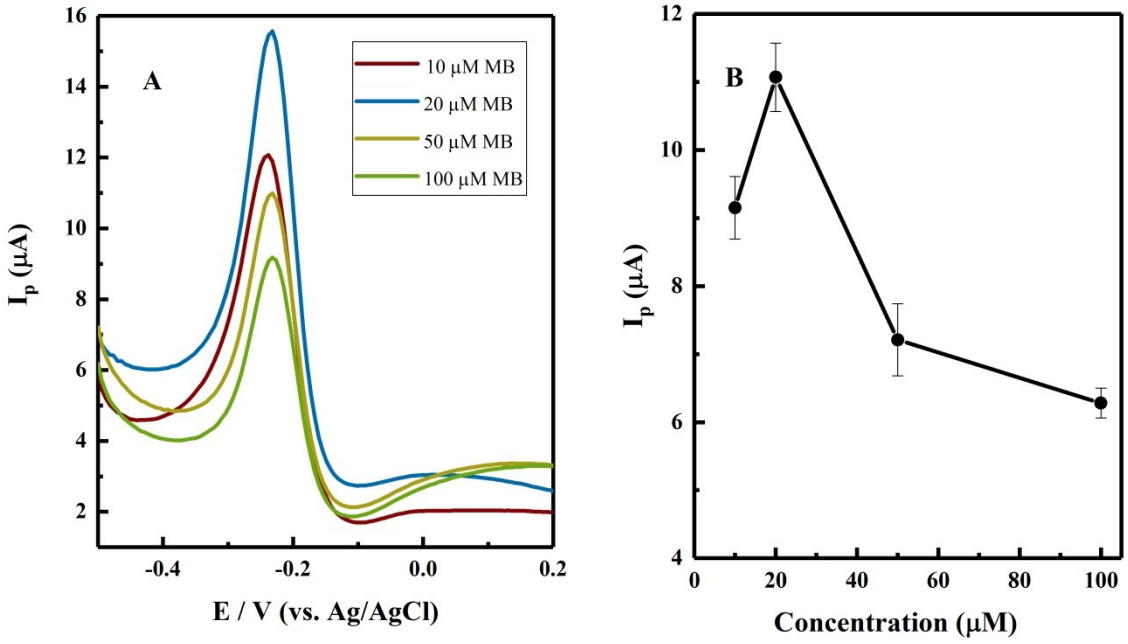
A
10 μM MB
20 μM MB
50 μM MB
100 μM MB
I_p (μA)
E / V (vs. Ag/AgCl)
B
I_p (μA)
Concentration (μM)

Fig. S9

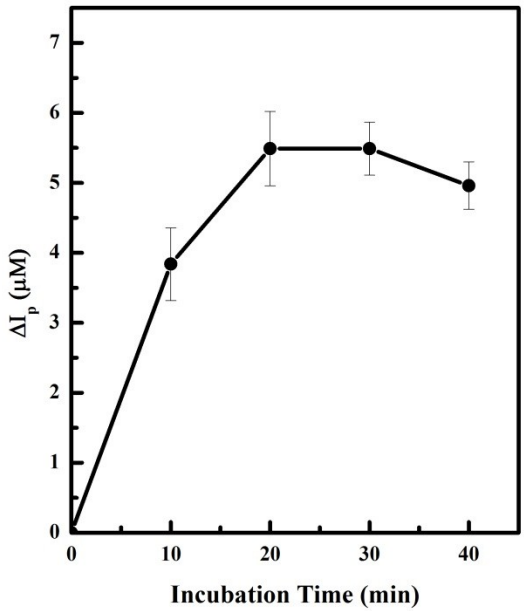

Fig. S10

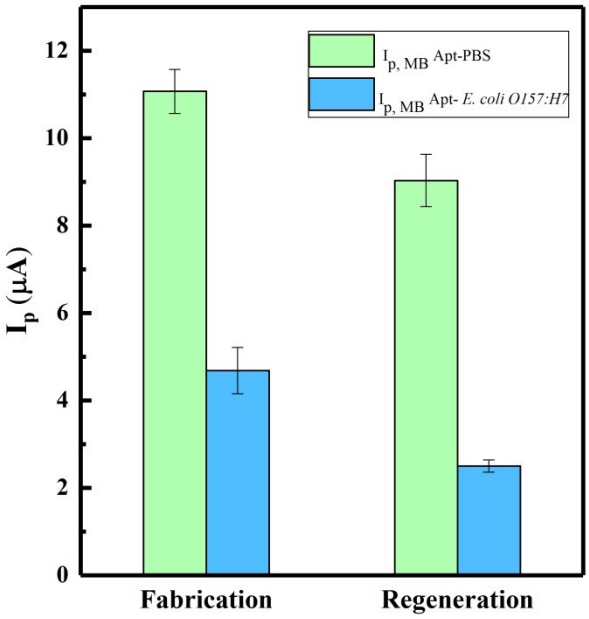
$I_{p, MB}$ Apt-PBS
$I_{p, MB}$ Apt- *E. coli O157:H7*
I_p (μA)
0
2
4
6
8
10
12
Fabrication
Regeneration

Fig. S11

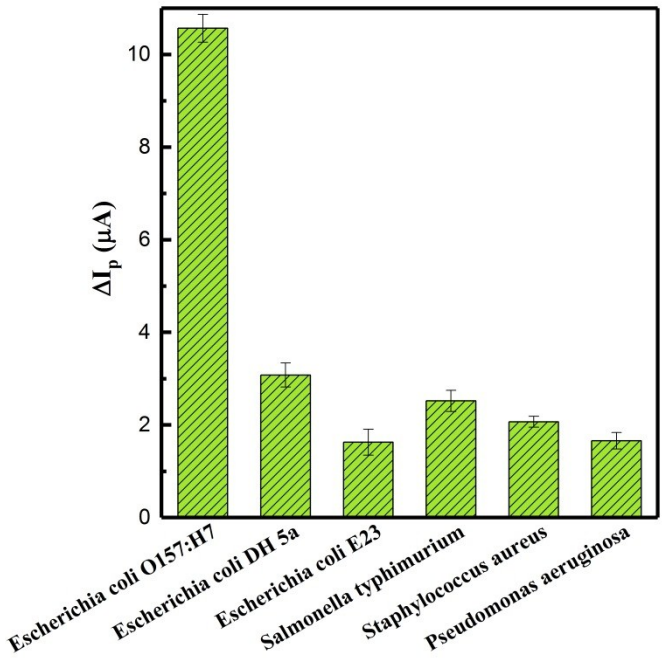
ΔI_p (μA)
0
2
4
6
8
10
Escherichia coli O157:H7
Escherichia coli DH 5a
Escherichia coli E23
Salmonella typhimurium
Staphylococcus aureus
Pseudomonas aeruginosa

Fig. S12

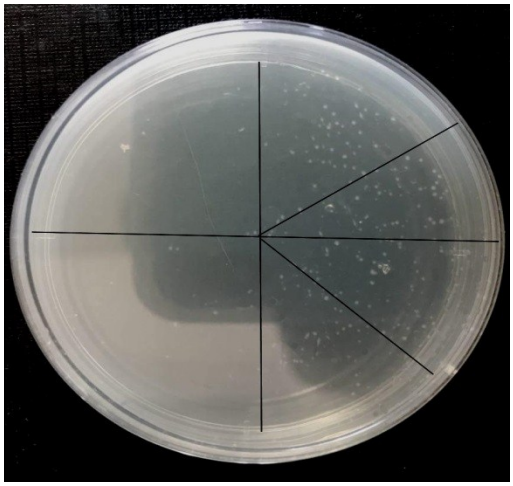

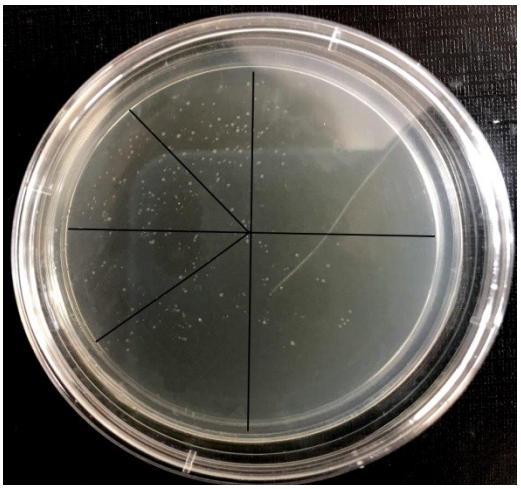

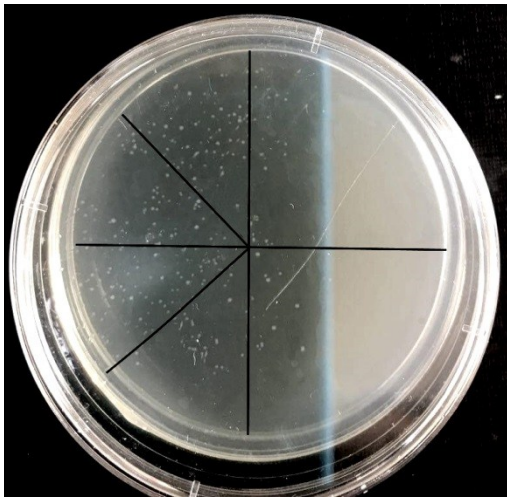

Fig. S13

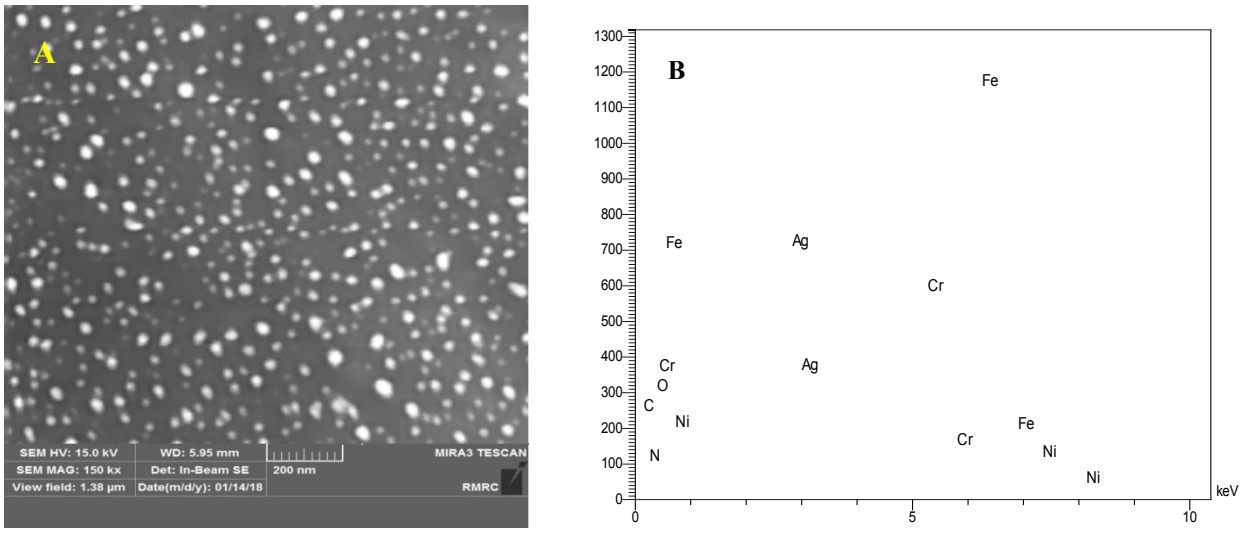

Fig. S14

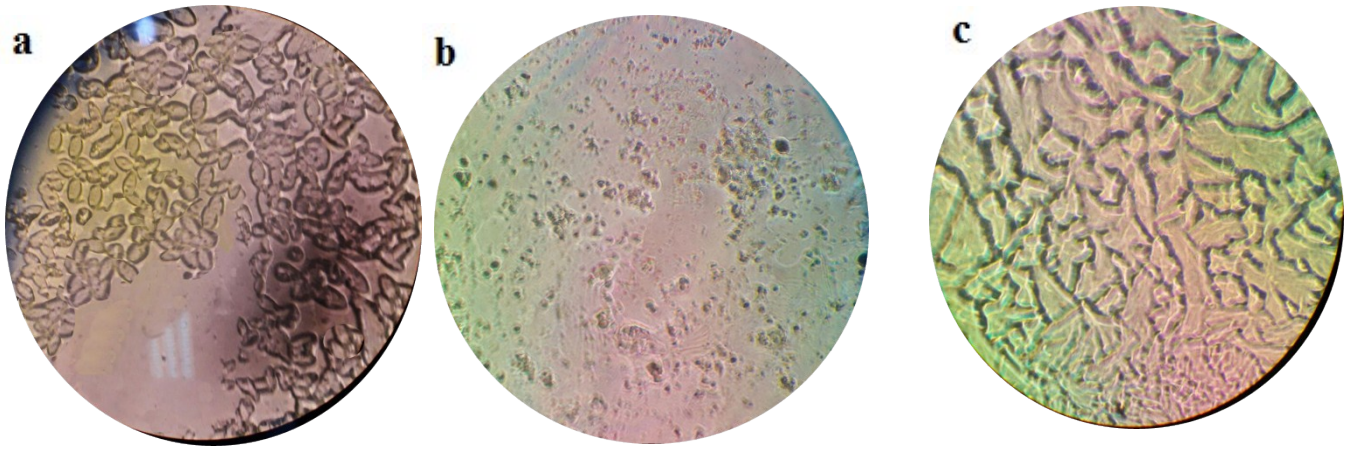

Fig. S15

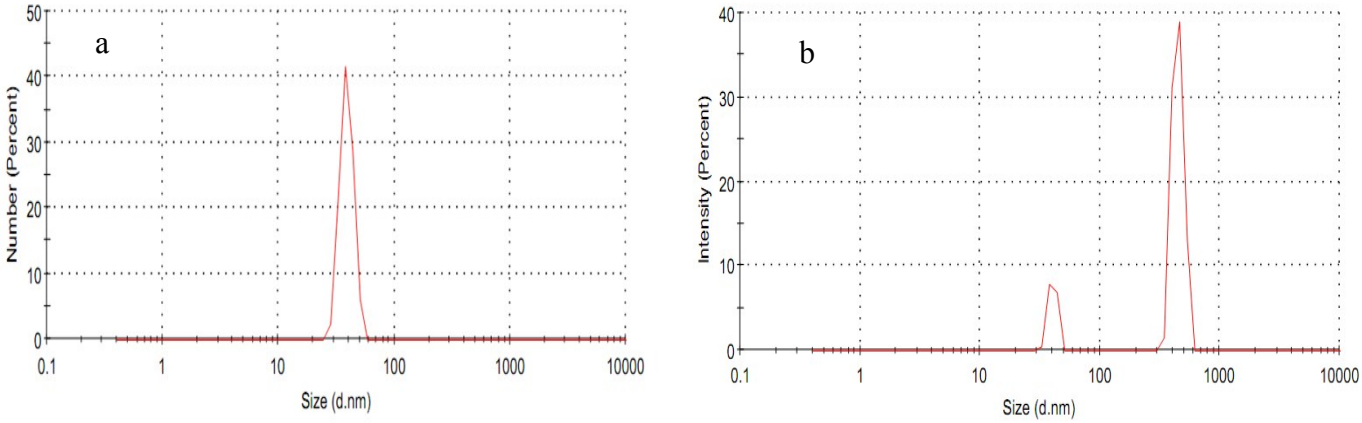
a
Number (Percent)
50
40
30
20
10
0
0.1
1
10
100
1000
10000
Size (d.nm)
b
Intensity (Percent)
40
30
20
10
0
0.1
1
10
100
1000
10000
Size (d.nm)

Fig. S16